Neural Comput & Applic (2018) 30:1203–1210
https://doi.org/10.1007/s00521-016-2716-7

ORIGINAL ARTICLE

Experimental and theoretical study of the color changes in OPP-based printing substrate on the gravure printing

Türkün Şahinbaşkan[1]

Received: 8 April 2015 / Accepted: 17 November 2016 / Published online: 9 December 2016

Abstract In this study, the color change performances of the prints that are made with gravure printing technique on OPP-based printing substrate used in food packaging are studied experimentally and modeled analytically using artificial neural networks. In this printing technique using solvent ink, small variations in the printing conditions and ink viscosity significantly affect the colors obtained as a result of the printing as the printing surface is not absorbent. In the test print made, samples were taken at certain intervals and color changes were determined with spectrophotometer measurements from test charts. The analytical relation giving the color changes based on the parameters they are linked to was obtained via artificial neural networks. Thus, the color deviations during normal production process shall be determined to ensure that necessary precautions are taken.

Keywords Gravure printing · OPP-based printing substrate · Artificial neural networks · CIE L*a*b*

1 Introduction

1.1 Gravure printing

Gravure printing technique is an intaglio printing technique. The regions to be printed are in shape of cells on the surface of the cylindrical printing plate. These cells are filled with high-fluidity, i.e., low-viscosity, ink. The excess ink is scraped from the plate cylinder with a steel scraper called doctor blade. The printing cylinder revolving at a high speed transfers the ink on the surface to be printed [1].

The structure of the printing cylinder is a copper-coated surface on steel. After it is rastered, the digital work prepared in the preprint stage is engraved on the copper surface via the diamond tips of the plate-preparation units, and this process is called engraving. There are different diamond tips for tram frequency and various depths of the ink-taking cells. After the engraving process, the surface is coated with nickel and surface strength is increased.

After the preparation processes are completed, the printing cylinders are mounted on the press and printing is started. In gravure print, especially high-circulation prints and flexible packaging prints are made. Although printing presses have usually eight color units, there are also ones with 16 units. Primer material comes in rolls and goes into printing. Gravure printing system is predominated with web system. The primer, on which ink is transferred in the printing unit, enters into the high-temperature drier unit and progresses to the next printing unit. After it passes through all the printing units, it is rewound into a roll in the output unit.

Gravure printing gives out a quality printing results. Wide color range and the clarity of the printed image are the most important advantages of the printing system. It is possible to achieve high printing speeds (180–400 m/min) due to rapid drying of the ink. Due to the robustness of the printing cylinder, high printing circulation can be achieved. Therefore, it is the preferred printing method for food and cleaning material packaging. In package printing, the substrate can be either various kinds of paper or film (transparent or opaque). In case of transparent films, the image can be printed on the front side and the reverse side for different purposes [2].

✉ Türkün Şahinbaşkan
turkun@marmara.edu.tr

[1] Department of Printing Technologies, School of Applied Sciences, Marmara University, 34722 Istanbul, Turkey

In the literature, there are studies by Kose [3, 4] regarding the use of ANN in the definition of color changes. In his study, Kose [3] defined amount of color change during drying in offset print using the ANN approach. He modeled the data obtained experimentally in this study with ANN. In the other study, Cengiz and Kose carried out the modeling of the rate that different eye colors perceive color using ANN. ANN has been very popular in the recent years due to its high accuracy in converting the experimental data of many problems into analytical approaches [5–7]. It is aimed, with this study, to define the color changes in OPP print obtained experimentally analytically depending on time using the ANN approach.

1.2 Printing substrate

Polypropylene (PP) is obtained via the polymerization of unsaturated hydrocarbons. Polypropylene has a high dimensional stability and provides optimum printing, cut, and applicability. Although it is less compressible than polyethylene, it provides superior clarity and is easily recovered. It is formed by subjecting it to heat and pressure after the base resin is reinforced with various additives. Thus, the film is obtained by stretching it at ratios of 1/16 and 1/18 at various stages laterally and longitudinally at various kiln temperatures.

The disadvantages of PP are that its elasticity is limited and that it is easily electrified (static electricity). The advantages of polypropylene can be listed as its high transparency, resistance to impacts and heat, its capability to be sterilized with steam (disinfection), good water vapor barrier, tear withstand at high tension, and printability after pre-processing.

Having a wide application, PP is generally used in light-food packaging, tobacco packaging, cooked food packaging, technical films, office products, medical and hygiene applications, and frozen food applications.

1.2.1 Types and structural properties

Having a non-oriented molecular structure, polypropylene may stretch more and cause problems in cutting. Therefore, nearly all of the polypropylene, which is used in the label sector due to its linear structure arising from the fact that additions can be made both in the flow direction and laterally on the production line, is BOPP, i.e. biaxially oriented polypropylene. This procedure gives the material a prefect printing control as well as a good clarity and a hardness that makes cutting easier. However, the material going through orientation process loses its elasticity.

There are two main types of polypropylene films: cast and stretched polypropylene. Cast polypropylene is formed, like polyethylene, by subjecting it to heat and pressure after the base resin is reinforced with various additives. The film is then obtained by stretching it at ratios of 1/16 and 1/18 at various stages laterally and longitudinally at various kiln temperatures.

Stretched polypropylene may be manufactured as mono-oriented or bi-oriented. While cast films have lower tear resistance, mono- or bi-oriented films have smoother surfaces, more hardness, and clarity.

Non-oriented polypropylene films have physical properties and printing character similar to low-density polyethylene films.

The chemical character of polypropylene is determined using catalysts and reaction conditions. The orientation process is the distinguishing property of OPP films. Chain molecules are aligned parallel and transversely in the printing press. The tension force of the oriented polypropylene is much greater than that of the non-oriented polypropylene. Orientation provides better clarity and elasticity at low temperatures. While OPP films are weak information in the machine direction, they are very strong in the transverse direction.

1.2.2 Printability criteria

When printing on OPP films with regard to flexo or gravure printing system, applications should be made based on the physical and surface properties of OPP. The surface property is important as it determines the attachment of the ink on the film surface. The surface tension of polypropylene is, as with polyethylene, lower than the value required for the ink to attach on the surface. In order for the ink to attach on the surface, surface tension is increased with corona process and made ready for printing process.

One of the most important factors in polypropylene film printing is the resistance to the elongation of the film in the machine direction. Because of the low surface energy of the polypropylene film, the film tends to elongate in the machine direction. Therefore, ambient temperature and temperature of the printing press are the factors to be considered in polypropylene film printing. As temperature rises, the resistance of polypropylene films decreases like in other thermoplastic substances (films). As the temperature that in polypropylene is subjected to (together with the mc temperature) approach 60 °C, the elongation of the material increases. When the material stretching during printing is considered, polypropylene elongates at a rate of maximum 6–7%. [8]

1.3 Gravure inks—solvent based, water based

Gravure inks are fluid inks with a very low viscosity that allows them to be drawn into the engraved cells in the

cylinder then transferred onto the substrate. In order to dry the ink and drive off the solvents or water, which essentially replace most of the solvent, the paper is run through gas-fired or electricity-fired driers. The ink will dry before the paper reaches the next printing station on the press. This is necessary because wet inks cannot be overprinted without smearing and smudging. Therefore, high-volume air dryers are placed after each printing station.

The solvent-laden air from the dryers is passed through either a solvent recovery system or a solvent vapor incinerator. A typical recovery system uses beds of activated carbon to absorb the solvent. Saturated beds are regenerated by steam. The solvent-laden steam is then condensed, and the water and solvent separate by gravity. More than 95% of the ink solvents can be recovered using this process (Buonicore). The solvents can either be reused or destroyed by incineration.

Water-based inks, especially ones used for packaging and product gravure, require a higher temperature and longer drier exposure time in order to drive off the water and lower vapor pressure constituents. As mentioned in the subsequent sections, flexo and gravure inks are very similar and the constituents are essentially the same. Again, a pollution control device may be needed [9].

1.4 CIE L*a*b* color model

The task of the International Commission on Illumination (CIE) is to create a color communication standards system that can be repeated for manufacturers of materials such as paint and ink. This is achieved by taking the human eye as a basis and using the color spectrum models that it produces. Providing a universal template for color matching is the main factor in these standards. While this template source is defined as a standard observer and XYZ color space, obtaining these standards is difficult, as shown in the XYZ chromaticity diagram, because of the out-of-balance nature of the XYZ space.

The L*a*b* color model uses quadrilateral coordinates that rest on the vertical yellow blue and green–red axis. It has developed better arranged color standards called CIE, CIE L*a*b*, and CIE L*u*v*. The well-balanced structure of L*a*b* is based on the theory that a color cannot be green and red or blue and yellow at the same time. Consequently, simple values can be used to describe red/green and yellow/blue attributes. L* lightness in CIE L*a*b* shows the value of a*red/green, b*yellow/blue (Fig. 1). This color space brings to mind three-dimensional color spaces such as the hue saturation lightless (HSL) color space.

Today, the most commonly used color space is the CIE L*a*b* color space which is also the space that all others are based on. In desktop publishing, computers and programs take the L*a*b* color system as a basis. CIE L*a*b* is the basic color space in the color management system [10].

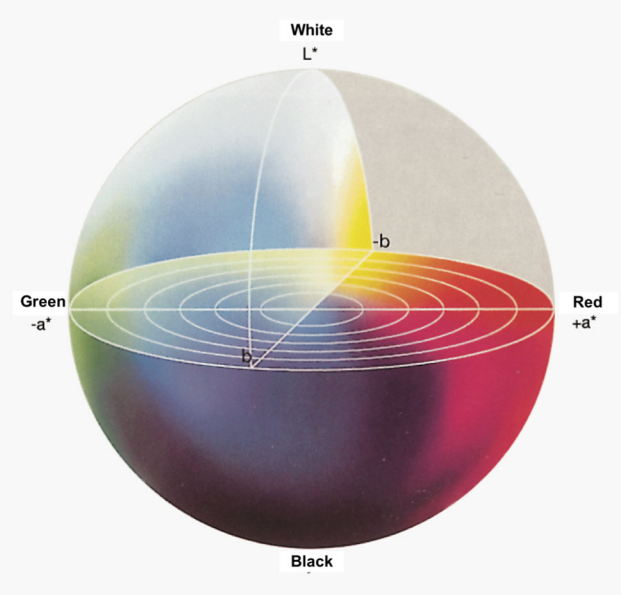

Fig. 1 CIE L*a*b* 1976 color model [11]

2 Material and method

2.1 Experimental studies

The primer material used was 114H/20-micron OPP film (Table 1). Media Wedge 2.× test chart was printed on 114H/20-micron OPP roll film material with gravure printing system using CMYK printing method. A print sample was taken every ten revolutions of the printing cylinder of 1 m perimeter, i.e. every 30 m. As a result of the print of 2000 m and the measurements made on 68 test charts with spectrophotometer, 46 CIE L*a*b* color values were obtained from 46 target color spaces. The color changes on the gravure print made on OPP film material using solvent inks were determined from these results.

2.2 Analytical modeling: artificial neural network technique

Artificial intelligence (AI) systems are widely accepted as a technology offering an alternative way to tackle complex and ill-defined problems [12]. They can learn from examples, are fault tolerant in the sense that they are able to handle noisy and incomplete data, are able to deal with nonlinear problems, and, once trained, can perform prediction and generalization at high speed [12]. They have been used in diverse applications in control,

Table 1 Technical properties of 114H/20-micron OPP used as primer material

Properties	Test method	Units	Actual values
Thickness	KGM-101	Micron	20.0 ± 0.8
Yield	KGM-103	m^2/kg	55.0 ± 2.3
Haze	ASTM D 1003	%	1.9 ± 0.5
Gloss	ASTM D 2457	%	95 ± 5
Dimensional stability (120 °C)	ASTM D 1204	%	MD −4.0 ± 1.0
			TD −2.0 ± 0.5
Tensile strength at break	ASTM D 882	kg/mm^2	MD 14 ± 2
			TD 30 ± 5
Elongation at break	ASTM D 882	%	MD 175 ± 15
			TD 50 ± 10
Coefficient of friction	ASTM D 1894	Film to film	FF 0.30 ± 0.05
			FB 0.30 ± 0.05
		Film to metal	FF 0.25 ± 0.05
			BM 0.25 ± 0.05
Wetting tension	ASTM D 2578	dyne/cm	38 ± 2
Heat seal range	KGM-104	C	FB 125
			BB 115

robotics, pattern recognition, forecasting, medicine, power systems, manufacturing, optimization, signal processing, and social/psychological sciences. AI systems comprise areas like expert systems, artificial neural networks, genetic algorithms, fuzzy logic, and various hybrid systems [12].

Artificial neural network is a system loosely modeled on human brain. In the brain, there is a flow of coded information from the synapses toward the axon. The axon of each neuron transmits information to a number of other neurons. The neuron receives information at the synapses from a large number of other neurons. According to Haykin [13], a neural network is a massively parallel-distributed processor that has a natural propensity for storing experiential knowledge and making it available for use. It resembles the human brain in two respects: the knowledge is acquired by the network through a learning process and interneuron connection strengths known as synaptic weights are used to store the knowledge [12]. ANN is an interconnected assembly of simple processing elements, units, or nodes, whose functionality is loosely based on the animal neuron. The processing ability of the network is stored in the inter-unit connection strengths or weights, obtained by a process of adapting to, or learning from, a set of training patterns [13].

A learning algorithm is defined as a procedure that consists of adjusting the weights and biases of a network, to minimize an error function between the network outputs, for a given set of inputs, and the correct outputs.

The back-propagation learning algorithm has been used in feed forward with a single hidden layer. Variants of the algorithm used in the study are the scaled conjugate gradient (SCG), Pola–Ribiere conjugate gradient (CGP) and Levenberg–Marquardt (LM). The LM algorithm with minimal error and maximal accuracy was achieved with three-layer network and six-neuron hidden layer. Neurons in the input layer have no transfer function. The logistic fermi function has been used.

The selected ANN structure that gives the least errors optimally is shown in Fig. 2. Each input is multiplied by a connection weight.

In the simplest case, products and biases are simply summed, then transformed through a transfer function to generate a result, and finally obtained output.

The error during the learning is called root-mean-squared (RMS) and defined as follows:

$$\mathrm{RMS} = \left((1/p) \sum_j \left| t_j - o_j \right|^2 \right)^{1/2} \tag{1}$$

In addition, absolute fraction of variance (R^2) and mean absolute percentage error (MAPE) are defined as follows, respectively:

$$R^2 = 1 - \left(\frac{\sum_j (t_j - o_j)^2}{\sum_j (o_j)^2} \right) \tag{2}$$

$$\mathrm{MAPE} = \frac{o - t}{o} \times 100 \tag{3}$$

where t is target value, o is output value, and p is pattern. Input and output layer are normalized in the (−1, 1) or (0, 1) range.

Fig. 2 Media Wedge 2.0 CMYK test chart used in spectral measurement

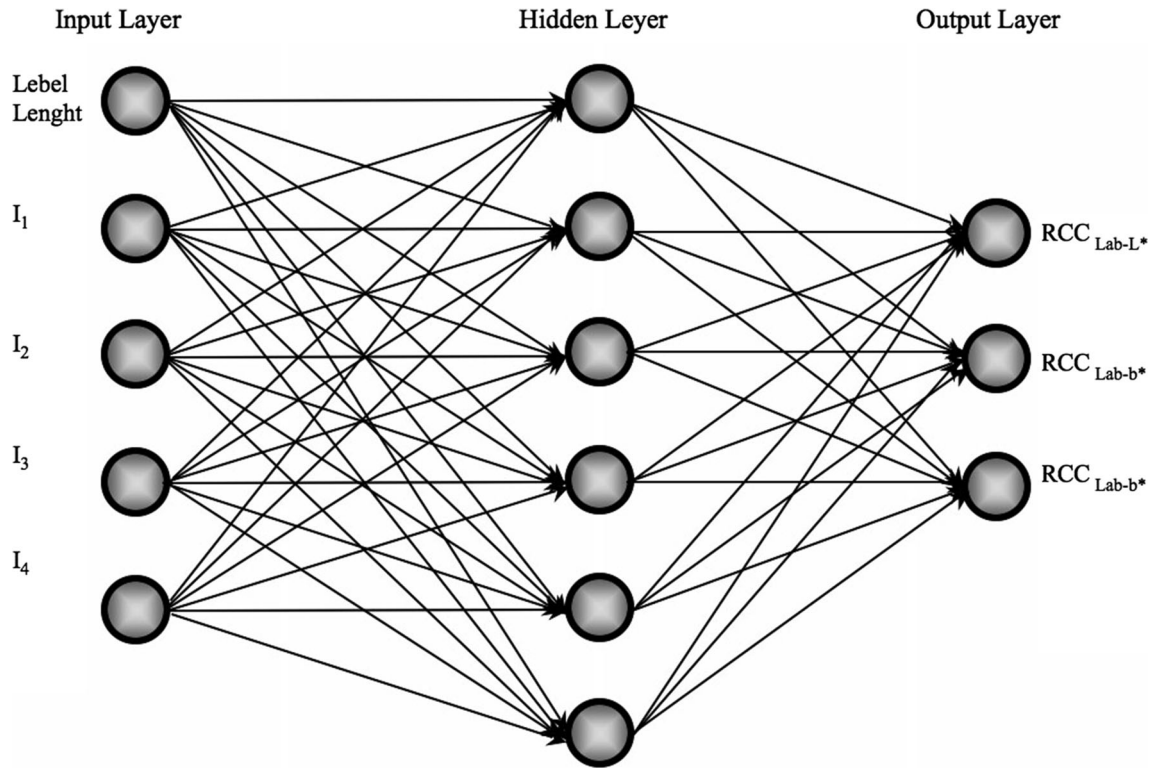

Fig. 3 ANN structure

3 Application and results

3.1 Experimental results

When evaluating the print results, the general average of the colors in the Media Wedge test chart and the L*a*b* color values at the regions where they make the highest deviations were taken into consideration. Along the 2000-m test print, the average values were very close especially in the first 100 m. In the second 1000 m, the difference began to increase. However, they were close to the color values specified in ISO 12647 and remained within the tolerances. When maximum deviations were considered, even if sudden rises were encountered at times at certain lengths, it was seen that the actual increases started in the second 1000 m. Some of these differences were above the tolerances specified in the ISO standard, and some were very close to the limits. Such color differences were observed especially in dark color tones where all four of the CMYKs were used. In monochrome prints and two-color mixtures, the differences between the colors were low.

3.2 Analytical results

The determination of the ratio for color changes (RCC) is made by the following equations:

$$\begin{aligned} \mathrm{RCC}_{\mathrm{LAB-L}} &= \text{First printer output}/\text{Experimental results} \\ \mathrm{RCC}_{\mathrm{LAB-A}} &= \text{First printer output}/\text{Experimental results} \\ \mathrm{RCC}_{\mathrm{LAB-B}} &= \text{First printer output}/\text{Experimental results} \end{aligned} \tag{4}$$

The estimated RCC are obtained using results of ANN application as shown in Fig. 3 modeling. The equations for the estimated each RCC values are given in Eq. 4.

Table 2 Constants (C_i) in Eq. 8

C_i	$RCC_{LAB\text{-}L}$	$RCC_{LAB\text{-}A}$	$RCC_{LAB\text{-}B}$
C_1	1.051962	0.513178	0.713225
C_2	2.927060	1.314429	0.750806
C_3	4.822033	1.859584	1.798020
C_4	−0.660038	−0.202823	−0.533668
C_5	0.838105	0.441146	0.397669
C_6	−0.677060	0.224960	0.174965

$$RCC_{LAB-L} = \frac{1}{1 + e^{-4(F_i - 0.5)}} \quad (5)$$

$$RCC_{LAB-A} = \frac{1}{1 + e^{-4(F_i - 0.5)}} \quad (6)$$

$$RCC_{LAB-B} = \frac{1}{1 + e^{-4(F_i - 0.5)}} \quad (7)$$

where F_i is given in Eq. 8. The C_i coefficients for Eqs. 5–7 are given in Table 2.

$$F_i = C_1 * N_1 + C_2 * N_2 + C_3 * N_3 + C_4 * N_4 + C_5 * N_5 + C_6 * N_6 \quad (8)$$

Equation 8 shall be used for the F_i value in Eq. 5. For the constants C_i in Eq. 8, the constants of the column RCCLAB-L in Table 2 shall be used. The N_i values in Eq. 8 shall be calculated using Eq. 7.

Similarly, in order to calculate the RCCLAB-A in Eq. 6, the F_i value shall be calculated based on Eq. 8, and to this end, the Ci constants of the column RCCLAB-L in Table 2 shall be used.

N_i can be calculated based on wavelength in Table 2 according to Eq. 8. Also, N_i are inputs of ANN structure.

$$N_i = \frac{1}{1 + e^{-4(E_i - 0.5)}} \quad (9)$$

where E_i can be calculated based on wavelength in Table 3 according to Eq. 10.

$$E_i = A_{1i}L_L + A_{2i}I_1 + A_{3i}I_2 + A_{4i}I_3 + A_{5i}I_4 \quad (10)$$

The constants (A_{ji}) in Eq. 10 based on wavelength are given in Table 3.

For example, we need E_1 value to calculate N_1. In order to calculate the E_1 value, Eq. 10 shall be used. In Eq. 10, the constants A_1, A_2, A_3, … of column N_1 in Table 3 shall be used to calculate the E_1 value.

The mean error in the color changes formulized by analytical solutions OPP-based primer materials during gravure printing is 1.7%. This value will help to predict the color changes with high accuracy without experimental studies.

The graphics clearly suggest that the ANN predictions are very close to the measurements. Since the ratio for color changes (RCC) obtained by ANN are very close to the actual values, they cannot be shown together graphically. For this reason, deviation values have been calculated by the following equation (Eq. (11)) and this has been shown graphically for the ratio for the deviations of color changes (d(RCC)) (Figs. 4, 5, 6) as percent (%). The maximum absolute deviations are 10% for d(RCC)LAB-L. When the y-axis is considered in Figs. 5 and 6, it is seen that the mean absolute error remains within the 1% limits.

$$d(\text{RCC}) = ((\text{RCC Actual} - \text{RCC}_{\text{ANN}}) * 100)/\text{RCC}_{\text{Actual}} \quad (11)$$

The deviations obtained for each of the three color changes are within acceptable limits. The usability of the obtained analytical relations for color changes has been ensured with high performance (Figs. 4, 5, 6).

4 Conclusion

It is observed that in terms of time, in the distribution of color, some colors get darker while others fade away. Analysis results show that neural network can be used to express color changes in time by depending on four colors (Figs. 5, 6). Figure 6 indicates that the model color change with neural network is possible by depending on the wavelength. As scientific studies are difficult, analytical modeling will lead the scientists.

- The advantages of the ANN compared with classical methods are speed, simplicity, and capacity to learn from examples.

Table 3 Constants (A_i) in Eq. 10

$\dot{I}$	N_1	N_2	N_3	N_4	N_5	N_6
A_1	2.472653	−0.048544	−0.344670	2.886647	0.157891	−2.942852
A_2	−6.552257	0.190548	0.029064	−7.904671	0.074033	−0.426939
A_3	−7.952323	−1.953835	−1.653083	−7.706432	6.548021	−1.145609
A_4	−6.395987	−1.302905	−0.680482	−7.588389	1.863146	−0.567645
A_5	−2.454409	−0.319841	−0.308425	−3.586029	−0.354452	4.787936

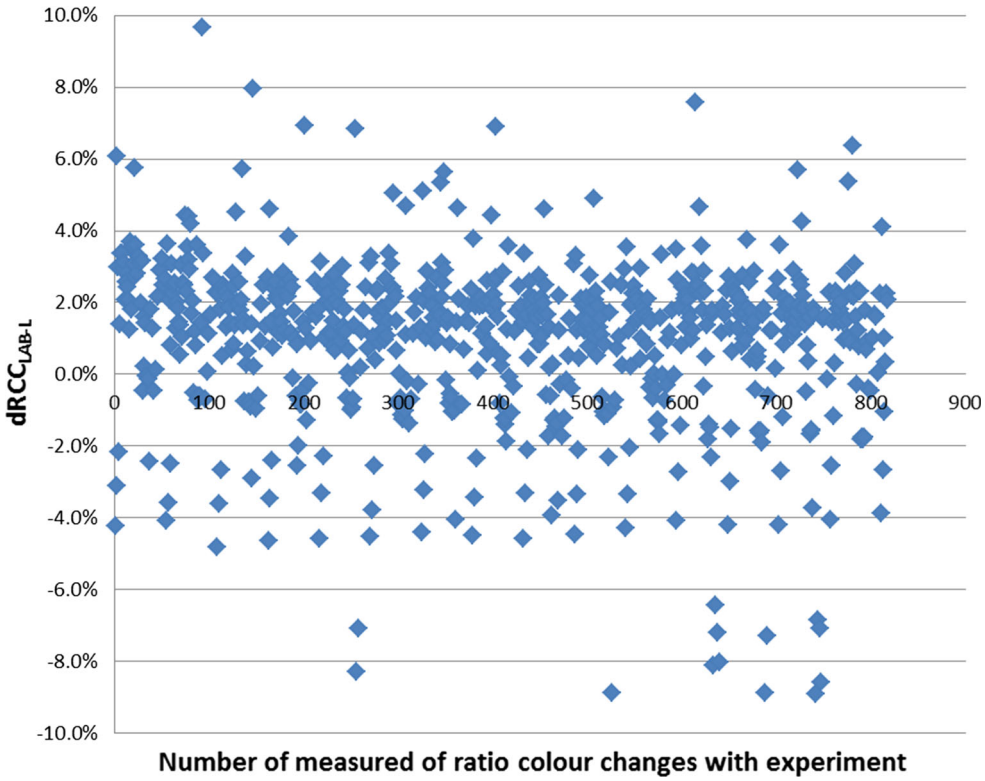

Fig. 4 Deviations for $RCC_{LAB\text{-}L}$

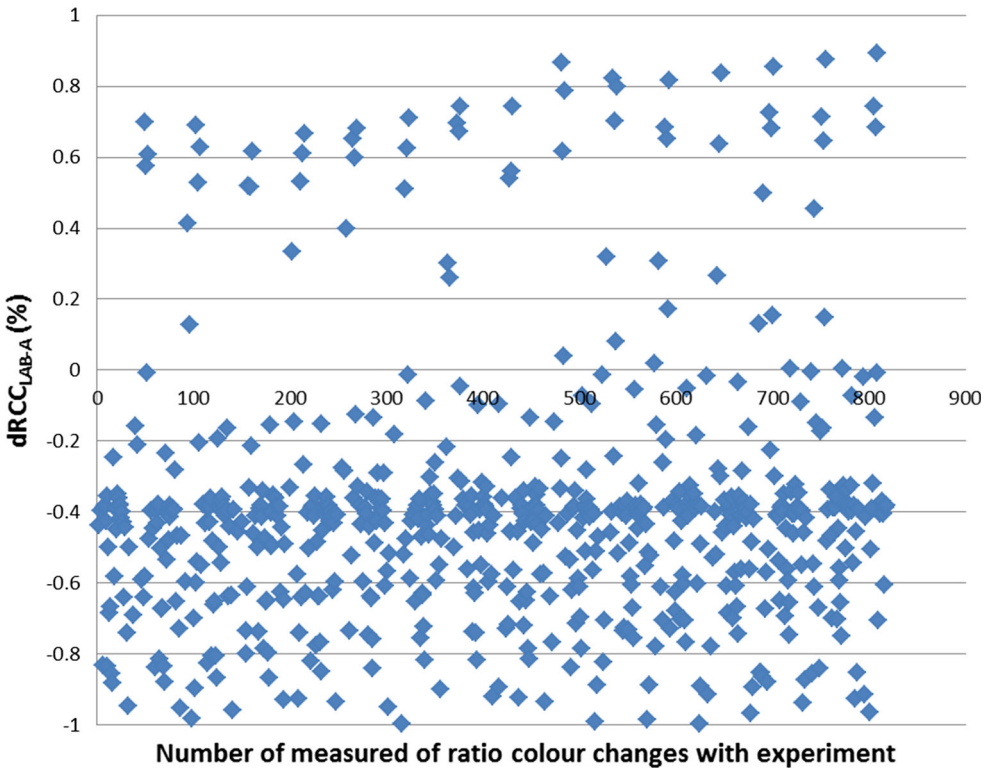

Fig. 5 Deviations for $RCC_{LAB\text{-}A}$

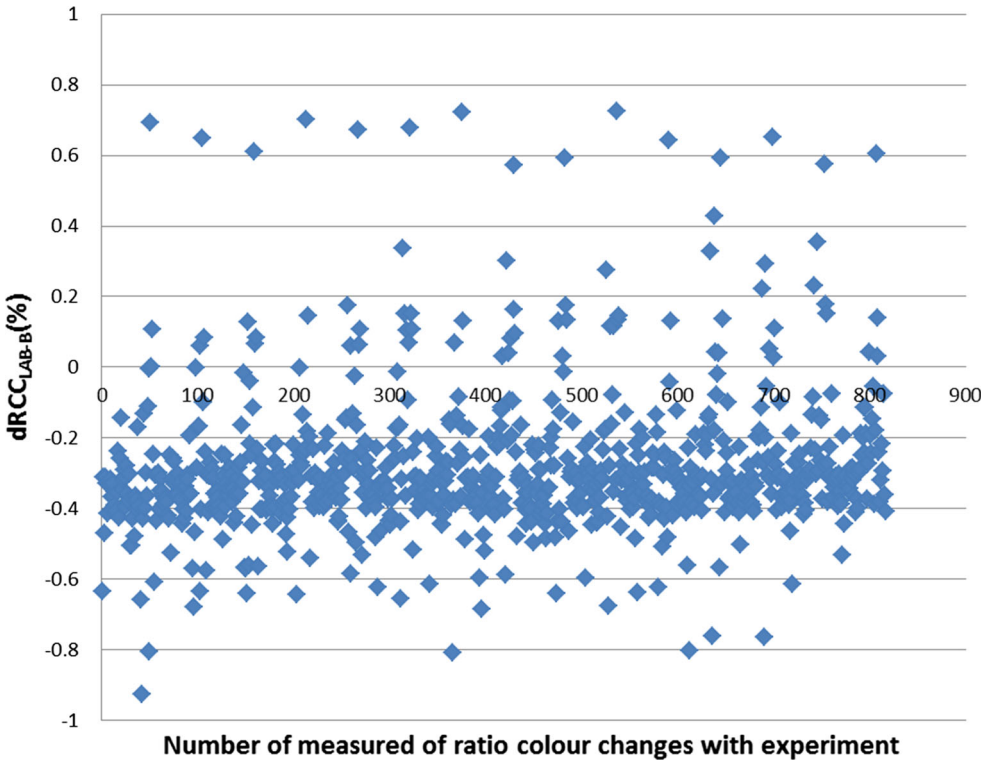

Fig. 6 Deviations for $RCC_{LAB\text{-}B}$

- This study is especially considered to be helpful in predicting the RCC.
- Results from neuronal model will allow improving determination of the spectral reflectance and understanding, in a short time, the behavior of the predicted analysis.

References

1. Hugh S (1998) Introduction to printing and finishing. Pira International, İngiltere. ISBN 1-85802-310-6
2. Gencoglu EN (2005) The effects of some engraving and film substrate parameters on the solid density and the dot gain in gravure printing. Surface coatings international part B: coatings transactions, vol 88, no 1, p 19. ISSN:1476-4865
3. Kose E (2014) Determination of color changes of inks on the uncoated paper with the offset printing during drying using artificial neural. Netw Neural Comput Appl 25:1185–1192
4. Cengiz C, Kose E (2013) Modelling of color perception of different eye colors using artificial neural networks. Neural Comput Appl 23:2323–2332
5. Srinivasan S, Ziad Saghir M (2014) Predicting thermodiffusion in an arbitrary binary liquid hydrocarbon mixtures using artificial neural networks. Neural Comput Appl 25:1193–1203
6. Srinivasan S, Ziad Saghir M (2013) Modeling of thermotransport phenomenon in metal alloys using artificial neural networks. Appl Math Model 37:2850–2869
7. MacKay DJC (1992) Bayesian interpolation. Neural Comput 4:415–447
8. Gençoğlu EN, Şimşeker O, Özdemir L (2009) Flekso Baskı Sistemi, Geliştirilmiş 2. Baskı. DuPont Türkiye, İstanbul. ISBN 978-9944-62-944-7
9. http://www.pneac.org/printprocesses/gravure/
10. Abhay S (2004) Understanding colour management. Thomson Delmar Learning, Stakmford
11. Stefan B, Liane M, Dietmar F (1999) Postscriptum on colour management. Gretag Macbeth
12. Sözen A, Gülseven Z, Arcaklıoğlu E (2007) Forecasting based on sectoral energy consumption of GHGs in Turkey and mitigation policies. Energy Policy 35(12):6491–6505
13. Haykin S (1994) Neural networks: a comprehensive foundation. Macmillan, New York